Journal of Entomology and Zoology Studies

Available online at www.entomoljournal.com

E-ISSN: 2320-7078
P-ISSN: 2349-6800
JEZS 2016; 4(1): 580-590

Received: 09-01-2016
Accepted: 11-02-2016

El habouz Youssef
IRF-SIC Laboratory,
University Ibn Zohr,
Agadir, Morocco.

Es-saady Youssef
IRF-SIC Laboratory,
University Ibn Zohr,
Agadir, Morocco.

El yassa Mostafa
IRF-SIC Laboratory,
University Ibn Zohr,
Agadir, Morocco.

Mammass Driss
IRF-SIC Laboratory,
University Ibn Zohr,
Agadir, Morocco.

Nouboud Fathallah
LIRICS, University Trois-Rivières, Québec, Canada.

Chalifour Alain
LIRICS, University Trois-Rivières, Québec, Canada.

El habouz Hammou
Laboratory of Biology and Ecology of the National Fisheries Research Institute (INRH) Morocco.

Manchih Khalid
Laboratory of Biology and Ecology of the National Fisheries Research Institute (INRH) Morocco.

Correspondence
El habouz Youssef
IRF-SIC Laboratory,
University Ibn Zohr,
Agadir, Morocco.

A new otolith recognition system based on image contour analysis

El habouz Youssef, Es-saady Youssef, El yassa Mostafa, Mammass Driss, Nouboud Fathallah, Chalifour Alain, El habouz Hammou and Manchih Khalid

Abstract
The external form of otolith is one of the main characteristics of fish species recognition; which is a major issue in several marine ecological studies; such as the determination of the food spectrum by the otoliths recovered from the stomach or feces. In this paper, we present an automatic identification system of fish species based on otolith shape analysis. Our proposed system consists of three main phases: pre-processing phase: image de-noising and enhancing grayscale contour. Feature extraction phase: we extract the median distance vector of the contour, which is used in the third phase, and this one is based on a multi-layer perceptron classification method. The efficiency of the new system was proved on two bases: AFORO database and a first national database, which is collected and prepared during the present work. Compared to Elliptic Fourier descriptors, Complex Fourier descriptors and Geodesic-based method, the correct recognition rate obtained was the higher, with 98.33 % for the first dataset and 95.6% for the second.

Keywords: Otoliths, Shape analysis, Fish species identification, Pattern recognition, Classification.

1. Introduction
Otoliths are concretions of calcium carbonate located at the inner ear of bony fish (Fig. 1). They are considered as a true biological and environmental archive to reconstruct the environmental parameters such as temperature, salinity. Otolith can be used to identify the life history traits of individual fish (e.g. age, reproduction, migration) [1]. Otolith has a distinctive external form according to the species as a result it is widely used in fish species identification [2, 3, 4]. The traditional approach for taxonomy, phylogeny and food-web studies of fish species is based on natural observation of the experts using the naked eye. However, this technique is extremely expensive and time consuming [5, 6]. Therefore, there is a demand of automated methods to identify fish species using otoliths. Automatic identification system of fish species is a big concern of several researches. Otolith based identification system is treated as an efficient tool in the analysis of stomach contents or feces (otoliths are slowly digested in the stomachs of some fish, fish-eating, cetacean and birds), to control the eating habits of fish and to conserve species that are threatened with extinction. Consequently looking for a quick, cheap and accurate method to recognize the fish species using otolith is crucial for the management of marine resources [7].

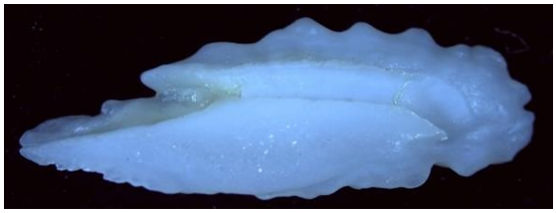

Fig 1: Otolith fish species of *Pagellus acarne*.

The computer viewing techniques offer a real opportunity for the identification of fish species using image analysis of otoliths. In this field, several methods have been proposed. The most popular method is shape analysis of otoliths based on Fourier descriptors [8]. These descriptors are computed from some equally spaced contour points. Elliptic Fourier descriptors method

(EFD) has been proposed to describe the complex shapes which contain the peninsulas and gulfs [9-13]. Wavelet transforms and representations of multi-scale curvature (CSS) approach are used on shape analysis of calcified structures [14-16]. Kamal Nasreddine proposed an approach based on the geodesic which is more preferment than EDF, with more significant otolith classification results [17].

The work present a new automatic recognition system of fish species based on otolith shape analysis. This system is composed of three principal phases: pre-processing, feature extraction and classification phase. The system was tested on several otolith images of various species, and proved a high performance compared to the most used approaches in this area of researches (complex Fourier descriptor, elliptic Fourier descriptor and based geodetic method).

2. Materials and methods

2.1 otoliths datasets

The system presented in this paper has been tested on two different otolith datasets, the first (DB1) was taken from the AFORO[1] website [7], the same database used in [17] and [18], the principal recent work in this field of research. The second (DB2) is the first original local otolith dataset from the Moroccan Atlantic area (Fig. 3) which acquired and prepared during our work.

DB1: this database content a set of 60 fish otolith images from AFORO database, consist of six species (namely, *Scomber colias, Coris julis, Umbrina canariensis, Diplodus annularis, Trachurus mediterraneus and Trisopterus minutus*), each species composed of 10 images (Fig. 2).

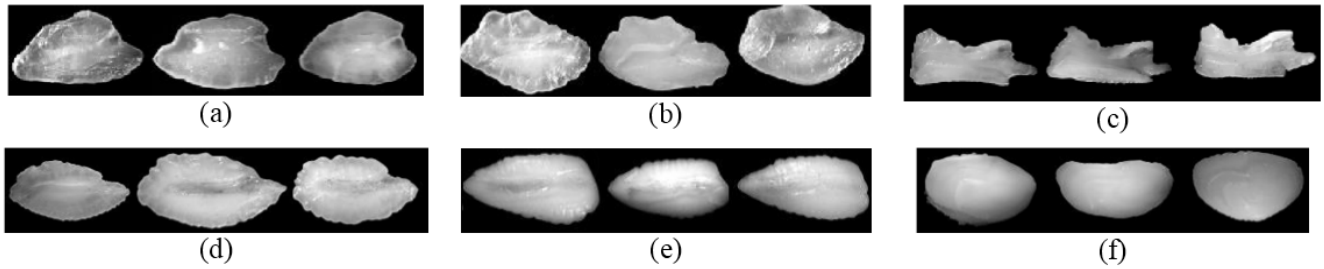

Fig 2: Examples of fish otolith images from Database DB1: (a) Coris julis, (b) *Diplodus annularis, (c) Scomber colias*, (d) *Trachurus mediterraneus* (e) *Trisopterus minutus* and (f) *Umbrina canariensis*

DB2: The otoliths samples used in this study are from the Moroccan Atlantic area between Larache in the north and Dakhla in the south (Fig. 3). These otoliths are collected by the National Institute of Fisheries research (INRH[2]) scientists, from 2002 to 2014, during biological sampling operations carried out on the research vessels and trawlers commercial landing. After the collection operation, we proceed to otolith acquisition process using the following tools: a stereo microscope Leica S8 APO, Leica camera EC3 connected to a PC and the Leica LAS EZ software (Version 3.0.0 for windows), the microscope is adjusted according to the otolith size, for a high resolution.

Fig 3: Map showing the study area between Larache in the north and Dakhla in the south.

The DB2 database contains 450 images from 15 different species, every species contains 30 images. In figure 4, we illustrate examples of otolith images in the database.

1. AFORO website: http://www.cmima.csic.es/aforo/.
2. INRH website: http://www.inrh.ma/

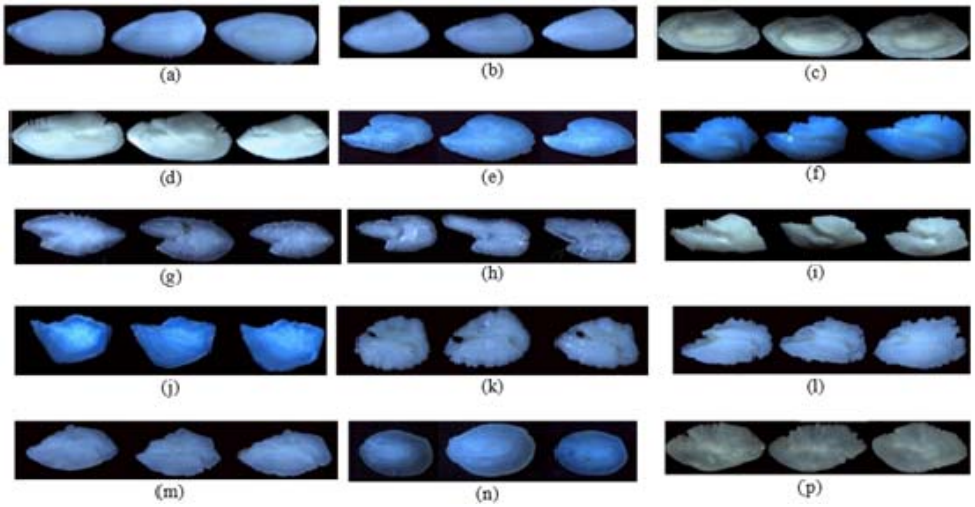

Fig 4: *Micromesitius poutassou*(**C2**), (b) *Merluccius merluccis*(**C3**), (c) *Merluccius polli*(**C12**), (d) *Merluccius senegalensis*(**C13**), (e) *Helicolenus dactylopterus*(**C8**), (f) *Trachurus trachurus*(**C9**), (g) *Engraulis encrasicolus*(**C10**), (h) *Sardina pilchardus*(**C11**), (i) *Trachyscorpia cristulata* (**C14**), (j) *Argentina sphyraena*(**C1**), (k) *Mullus surmuletus*(**C4**), (l) *Pagellus acarne*(**C5**), (m) *Pagellus erythrinus*(**C6**), (n) *Dicologoglossa cuneata*(**C7**), (p) *Plectorhynchus mediterraneus*(**C15**).

Among the chosen species, there are many species, which the shape otolith is almost similar. For example C2, C3, C12 and C13; or the group of C10 and C11; and the group C8, C9, C14, C1, C5, C6, *and C15,* and the group *C4, C7.* This similarity makes the problem more challenging and adjusted to real working conditions.

2.2 Proposed System

The following system is based on shape analysis of otolith in order to control the management of marine resources. First of all an input otolith image is given to the preprocessing phase which contains three steps: filtering, contour detection and otolith contour orientation step. The feature extraction phase consists on the extraction of the median distances of the contour. The classification phase is the last one, based on a multi-layer perceptron classification method, this phase give us an otolith class as an output.

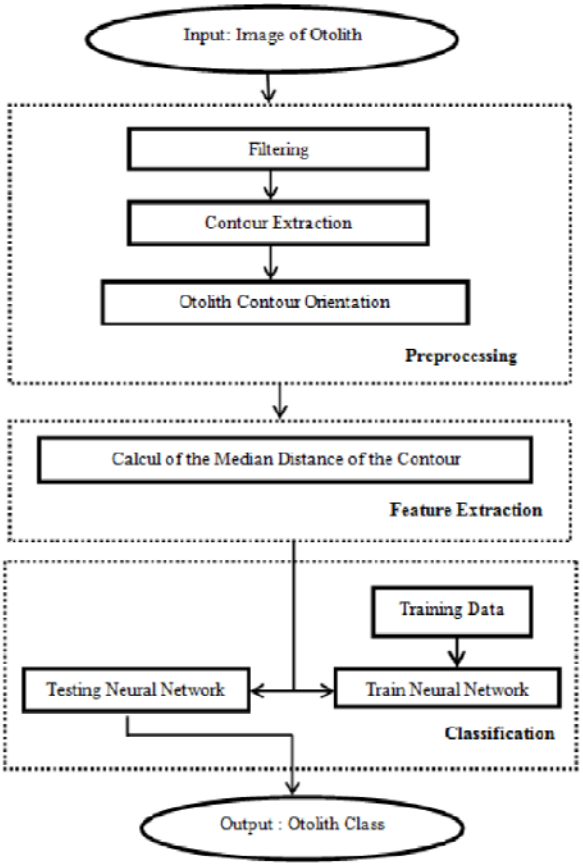

Fig 5: System architecture

In the paragraphs below we will focus on the main steps of the proposed system, for each step, the main principal and the related functionality are presented.

2.2.1 Contour Extraction

Edge detection techniques are widely used in image processing, in different areas from the data compression, image enhancement to pattern recognition. The main contribution of these techniques is to characterize the semantic information contained in the image independently of the background, (Example: contours of otolith image). These methods are often preceded by a prefiltering. In our proposed system we used the mean filter and mathematical morphology operators [19] (Fig. 6). Afterward we trace the contour of otolith using a threshold method (see algorithm 1) in order to extract the pixels belonging to the contour [20].

(a)

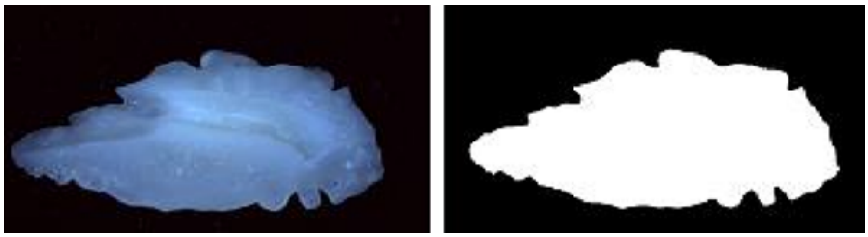

(b)

Fig 6: Results after applying the mean filter and mathematical morphology operators to the original image: (a) Otolith of *Trachyscorpia cristulata* and (b) Otolith of *Pagellus acarne*

Thresholding algorithm:

Algorithm 1:

```
INPUT:
    A is the original image;
OUTPUT:
C: a set of pixel;
BEGIN
        Af←the image A filtered; a1, a2 ,
        a3, a4← to be determined;
        FOREACH pixel P=Af(x,y)IN Af
                IF  a1 <gray level P< a2 THEN
                        C(x,y)←255; (The pixel is not a contour point (white))
                ELSEIF a3 <gray level P < a4 THEN
                        IF the grey level of one of its -connected neighbor  is between a1 and a2 THEN
                                C(x,y)←0; (the pixel is a contour point (black))
                        ELSE
                            C(x,y)←255;(the pixel is not a contour point (white))
                        ENDIF
                ENDIF
        ENDFOR
END
```

In an image of NxM pixels, the background is clearly different from the Otolith itself. We suppose that the grey level background value is between a1 and a2, and the value of the otolith pixels is from a3 to a4. (a1, a2, a3 and a4 are fixed values). The pixel belongs to the contour, if the grey level of one of its neighbors is between a1 and a2. The contour extraction method is representing in the algorithm below. In the Figure 7, we present an example of the results of otolith contour extraction method.

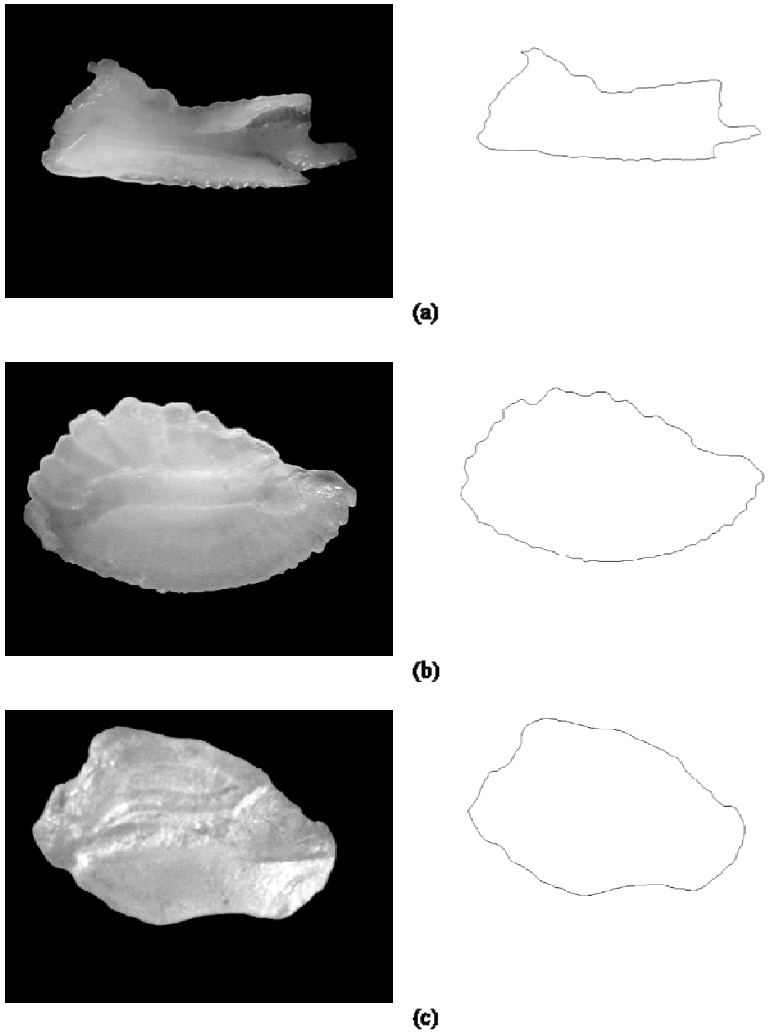

Fig 7: Otolith contour extraction : -(a) in the left: Otlolith specie of *Scomber colias* and in the right the contour extraction. -(b) In the left: Otlolith specie of *Trachurus mediterraneus* and in the right the contour extraction. -(c) in the left: Otlolith specie of *Diplodus annularis* and in the right the contour extraction.

2.2.2 Otolith Contour Orientation

The aim of this step is to make a standard orientation for all otoliths images contour.

After contour extraction, we detect the principal axis (AB) of the otolith contour:

C represents the outline of an otolith.

A= (X_a, Y_a) and B= (X_b, Y_b) are two points belong to the contour.

The distance AB is the maximum distance between two points of C.

X_a, X_b and Y_a, Y_b are the horizontal and vertical coordinates of A and B respectively.

To calculate the distance AB we use the Euclidian distance (below the formula 1).

$$|AB| = \sqrt{(Xb - Xa)^2 + (Yb - Ya)^2} \quad (1)$$

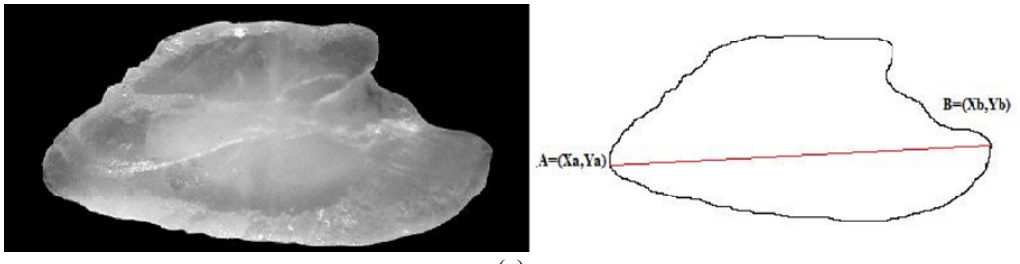

(a)

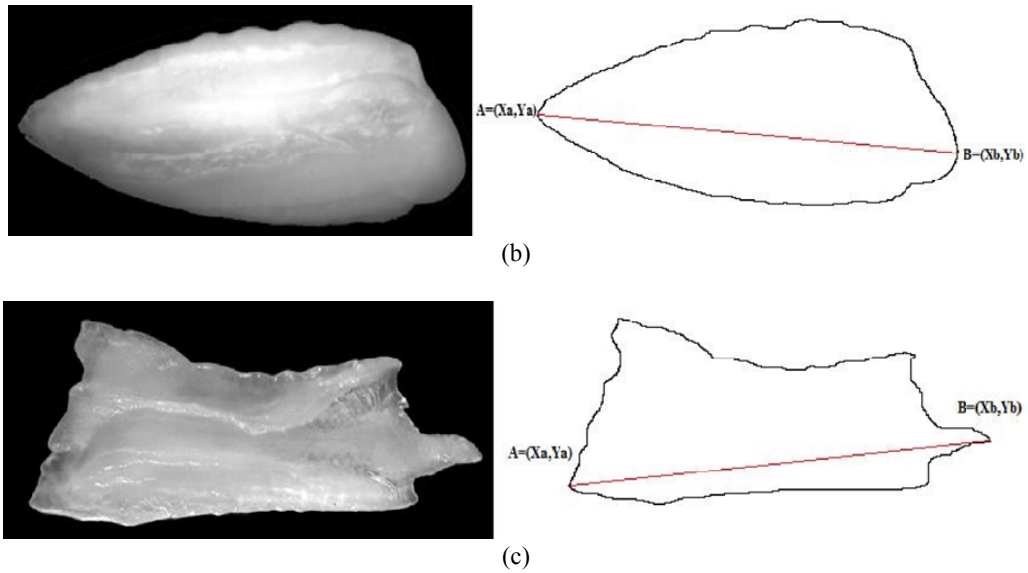

Fig 8: The principal axis of the otolith contour: (a) *Coris julis*, (b) *Scomber colias* and (c) *Trisopterus minutus*.

We calculate Θ (the angle between the major axis and the horizontal axis of contour C) using formula (2):

$$\theta = \arcsin(|Xb - Xa|/|AB|) \qquad (2)$$

Let |AB| the maximum distance between two points A and B in C.

$$A = P(x_a, y_a) \text{ and } B = P(x_b, y_b).$$

The segment AB is the main axis of the otolith (Fig. 8).

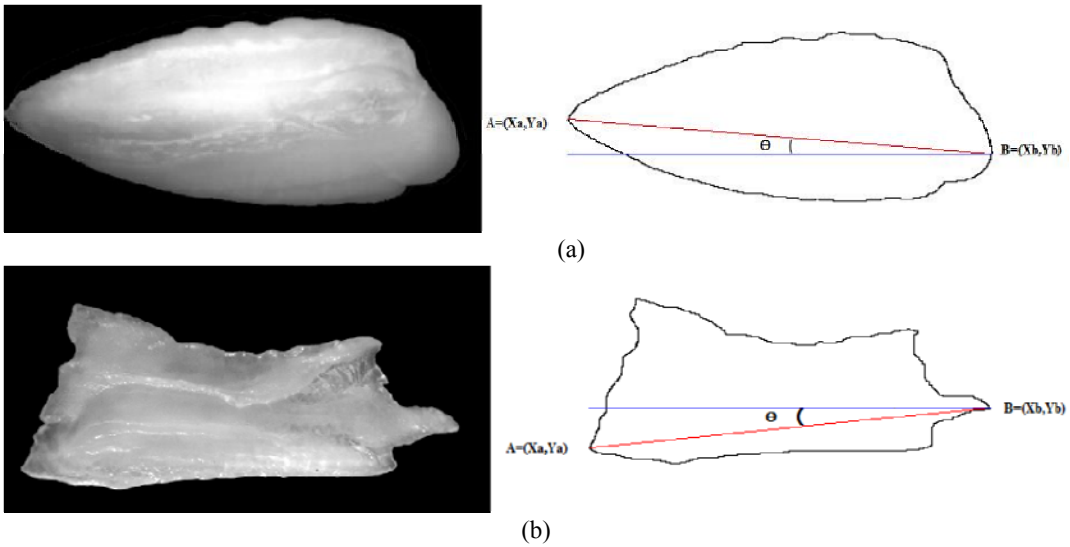

Fig 9: The angle between the vertical and the principal axis of the otolith contour, (a) *Trisopterus minutus* and (b) *Scomber colias*.

If θ is not null, Then a contour rotation is needed (Fig 9).

The angle Θ is used to perform a rotation of contour C. B= (X_b, Y_b) is the center of rotation (Algorithm 2).

Algorithm 2:

INPUT:
C: all coordinate points (X, Y) forming the contour of the otolith
OUTPUT :
C': the transformation results which we wants to perform
BEGIN:
AB←the principal axis of C;
A=(X_a,Y_a)←the first point of the major axis AB ;
Θ←the angle between AB and the horizontal axis of contour C.
IF $\Theta \neq 0$
For each point P=(X,Y) **from** C
IF $X=X_b$ **and** $Y=Y_b$
$X' \leftarrow X_b$;
$Y' \leftarrow Y_b$;
ELSE
$L \leftarrow Y_b - Y$;
$D \leftarrow \sqrt{(X - X_b)^2 + (Y - Y_b)^2}$
$T \leftarrow \arccos(D/L)$;
IF ($X_a < X_b$) the rotational direction
$\Theta' \leftarrow T - \Theta$;
ELSE
$\Theta' \leftarrow T + \Theta$;
ENDIF
$X' \leftarrow Xb - d * \sin(\Theta')$;
$Y' \leftarrow Yb + d * \cos(\Theta')$;
ENDIF
ENDFOR
ELSE
C'←C ;
ENDIF
We take $n \geq \min(X')$ and $m \geq \min(Y')$; (X', Y') is a point belongs to C'

FOR EACH P'(X', Y') **FROM** C'

IF ($X' < 0$ or $Y' < 0$)
$X' \leftarrow X' + n$;
$Y' \leftarrow Y' + m$;
ENDIF
ENDFOR
END

2.2.3 Vector median distance of the otolith contour

The purpose of this step is to calculate the distances vector of the contour C; which is used in recognition phase. For each contour C we divide equally the main axis (AB) to n+ 1 sub-segment.

Let $\mathbf{S = \{A = S_1; S_2, S_1, \ldots, S_{n+1} = B\}}$, the set of pixels belongs to the segment AB. The distance between two pixels S_t and S_{t+1} is $\mathbf{D_n = \frac{|AB|}{(n+1)}}$.

The length of each sub segment $[S_t S_{t+1}]$ is related to the value of n. (see proof 1).

For a significant subdivision S we selected n such that: $\mathbf{9\ pixels \geq D_n \geq 1 pixels}$.

The value of n belongs to the interval $\left[(|AB|) - 1, \quad \frac{(|AB)|-9}{9}\right]$.

Proof 1:
We consider the distance D_n as a sequence D(n) defined by:
$D(n) = \frac{|AB|}{(n+1)}$, $\forall n \in N - \{0\}$ with N is the set of the natural numbers
We have:
$\frac{D(n-1)}{D(n)} = \frac{n}{n+1} = 1 + \frac{1}{n} > 1, \forall n \in N - \{0\}$ (D (n) is a decreasing sequence) and $\lim_{n \to +\infty} D(n) = 0$
Consequently the increase of n implies the decrease of D (n)

St_i and Sl_i are the intersection between the vertical axis on S_i and the contour in two side top and low. From these distance values we construct the vector $V = \{Dt_1, Dt_2, Dt_3, \ldots, Dt_n\}$. We normalize the V vector on dividing each component by |AB| to make this approach invariant to the scale change. For each image, the vector of distances V is extracted. V is used for training Neural Network in the classification phase.

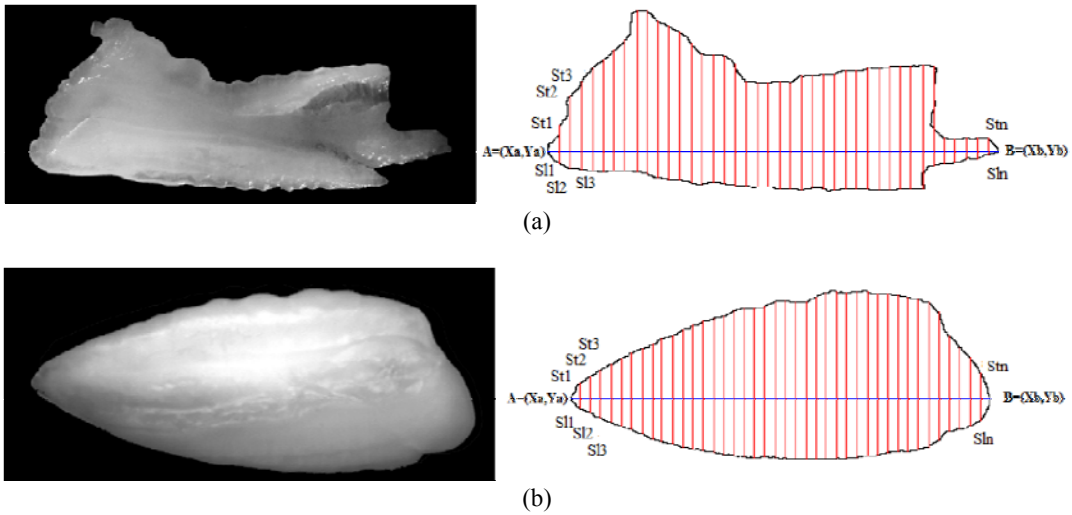

Fig 10: Median distance contour of Otolith: (a) *Scomber colias* and (b) *Trisopterus minutus*.

We show in Figure 10 a real example of the vector distances extraction: Figure.10 (b) *Trisopterus minutes* otolith species. The number of subdivision in this example is n=40, in this case the length of the vector c is 40 elements with: $V = \{Dt_1, Dt_2, Dt_3, \ldots, Dt_n\}$.

2.2.4 Classification

There are several available architectures and learning methods. The choice of these methods is related to the kind of the problem. In this paper, we choose a multi-layer perceptron architecture using the back propagation gradient network [21, 22]. This network consists of three or more neuron layers: input layer, output layer and at least one hidden layer. In most cases, a network with only one hidden layer is used to restrict the calculation time, especially when we obtained an efficient results [23]. The Figure.11 presents the Artificial Neural Networks (ANN) Architecture. The NN comprised 40 input neurons (number of features), 15 output neurons (number of classes) and the number of neurons in the hidden layer was empirically determined. Every neuron of each layer (except the neurons of the last one) is connected to the neurons of the next layer (Fig. 11). The network was trained with the available data. The combination of output vector and known input is called learning sample. The predicted output is compared with the known value. The weights on the arcs are adjusted depending to the prediction of the actual result. At each stage the sigmoidal transfer function is used for generating an output.

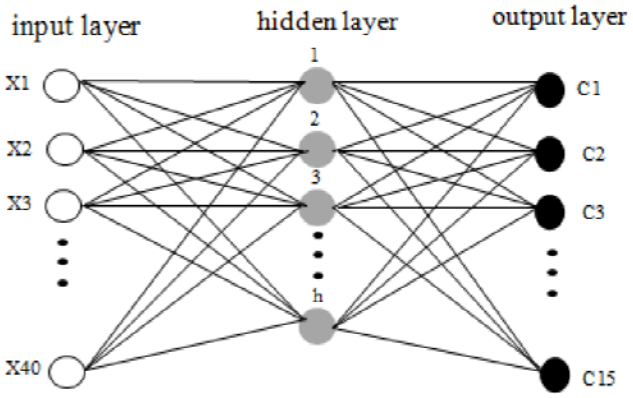

Fig 11: ANN Architecture (three layers: input, hidden and output)

3. Experimental results

We have tested the proposed system on two databases of otolith: a database taken from AFORO (DB1) and the first Moroccan otolith dataset (DB2). We presented the two datasets previously in the section (2). The first tests were carried out on the DB1 database in order to choose the optimal value of the n, where n is the subdivision number of the otolith contour main axis. n varied from 10 to 100, and for each value of n we calculated the classification rate. Figure 12 presents the results of this first test, we note that the classification rate was stable since n = 40. To optimize the calculation time of the distances vector we opted to n = 40.

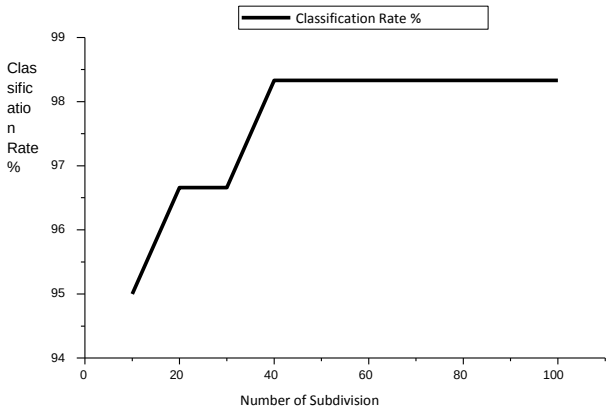

Fig 12: Classification rate of the database DB1 by the number of subdivision of the main axis of the otolith

We presented a comparative study of our proposed system results on DB1 dataset (Table 1), and the results of the most methods on fish species classification, presented in [17]: complex Fourier descriptor, elliptic Fourier descriptor, based geodetic method. The results present the number of otolith correctly identified from the total otolith number of each class. Using our system, we obtained a smaller misclassifications rate (1.66% using Euclidean distance, 3.33% using shape geodesics, 15% using elliptical Fourier descriptors and 18.34% using complex Fourier descriptors). The proposed approach recognizes all otolith species of the experiment on DB1 dataset except one sample of *Trachurus mediterraneus* otoliths, which are not correctly classified. This shows that the classification metric proposed offer a significant improvement to the recognition performance.

Table 1: The results of the proposed system and the most preferment methods on classification of fish species

	Methods			
Fish species	Complex Fourier descriptor	Elliptic Fourier descriptor	Geodesic-based method	Our system
Coris julis	10/10	7/10	10/10	10/10
Diplodus annularis	6/10	8/10	10/10	10/10
Scomber colias	9/10	9/10	10/10	10/10
Trachurus mediterraneus	6/10	10/10	8/10	9/10
Trisopterus minutus	9/10	9/10	10/10	10/10
Umbrina canariensis	9/10	8/10	10/10	10/10
Rate of Correct Classification	81.6%	85%	96.7%	98.33%

For the experiment of DB2 dataset, the classification results are reported in table 2. We have used 70% of images for training the neural network, 15% for testing and 15% for validation. Figure 13 shows an efficient validation results. The recognition rate is 95.6%.

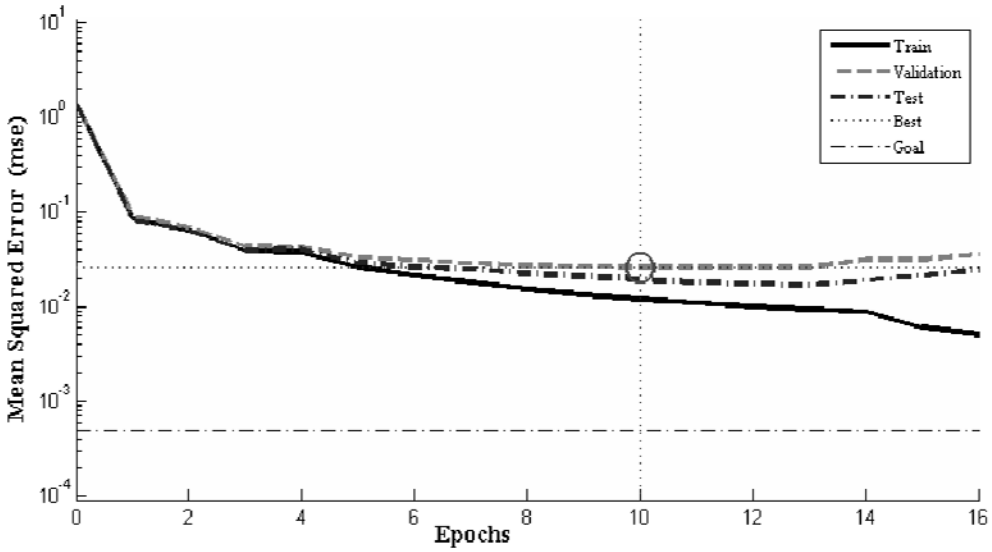

Fig 13: Validation results after training: the Best Validation Performance is 0.025764 at epoch 10

The table 2 below presents the confusion matrix of the system on DB2. The study of this confusion matrix showed that the most misclassified otoliths are mainly due to the resemblance between some otoliths shape (Fig. 14). For examples, the first confusions are between the species of the *Merluccius* genus: 25 images of C3 are properly classified, four images of the same class are recognized as C13 and one recognized as C12. 23 otoliths of C13 are correctly classified; two images of this class are recognized as C12 and five as C3.

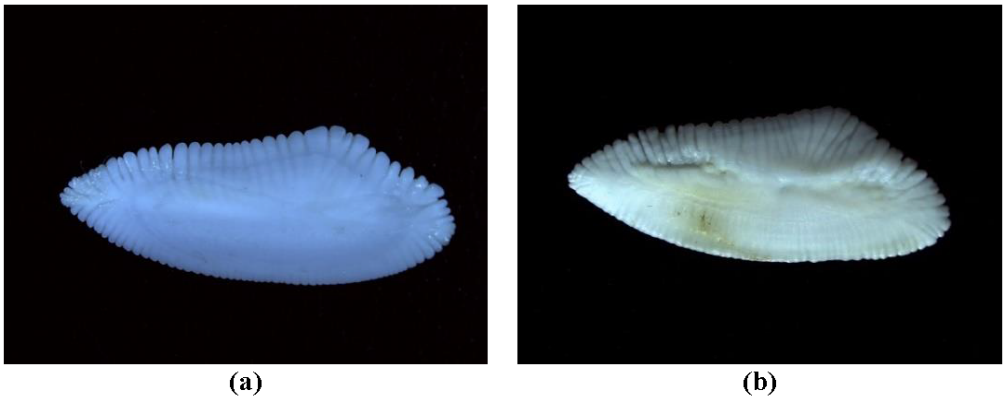

Fig 14: Example of resemblance between some otoliths shape: *(a) Merluccius merluccius* ans (b) *Merluccius senegalensis*

The other problem is due to the difficulty of otolith extraction from the fish (otoltih broken) (Fig. 15), this causes the resemblance between otolith shape. For examples: 27 images of *Pagellus acarne* (C5) are correctly recognized, three images of this species are misclassified, one recognized as C6, the second as C2 and the last one recognized as C8.

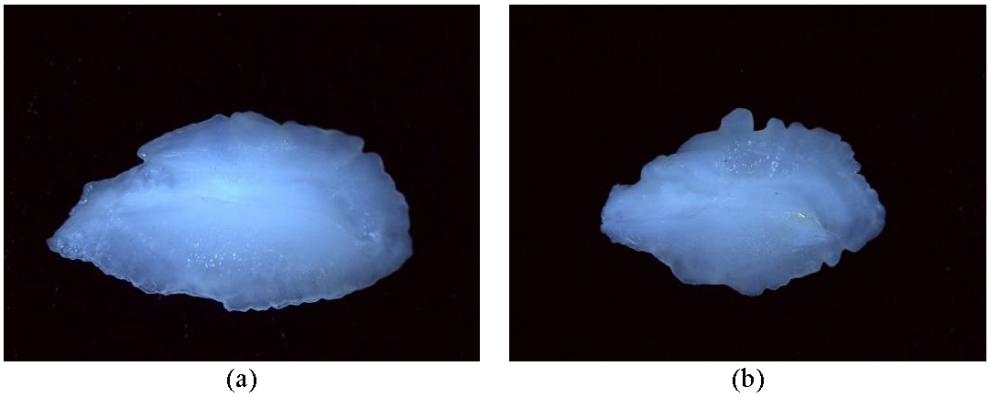

Fig 15: Example of otolith broken: (a) *Pagellus acarne* and (b) *Pagellus erythrinus*.

Table 2: Confusion matrix of the system on database DB2

Actual class	Estimated class														
	C1	C2	C3	C4	C5	C6	C7	C8	C9	C10	C11	C12	C13	C14	C15
C1	30	0	0	0	0	0	0	0	0	0	0	0	0	0	0
C2	0	30	0	0	0	0	0	0	0	0	0	0	0	0	0
C3	0	0	25	0	0	0	0	0	0	0	0	1	4	0	0
C4	0	0	0	29	0	1	0	0	0	0	0	0	0	0	0
C5	0	1	0	0	27	1	0	1	0	0	0	0	0	0	0
C6	0	0	0	0	0	30	0	0	0	0	0	0	0	0	0
C7	0	0	0	0	0	0	30	0	0	0	0	0	0	0	0
C8	0	0	0	0	0	0	0	30	0	0	0	0	0	0	0
C9	0	0	0	0	0	0	0	0	29	0	0	0	0	1	0
C10	0	0	0	0	0	0	0	0	0	30	0	0	0	0	0
C11	0	0	0	0	0	0	0	0	0	1	29	0	0	0	0
C12	0	0	0	0	0	0	0	0	0	0	0	29	0	0	1
C13	0	0	5	0	0	0	0	0	0	0	0	2	23	0	0
C14	0	0	0	0	0	0	0	0	0	0	0	0	0	29	1
C15	0	0	0	0	0	0	0	0	0	0	0	0	0	0	30

4. Conclusion

In this paper, we have presented an automatic recognition system of fish species, based on three principal phases: pre-processing, feature extraction (vector of Euclidian distances) and classification (Artificial Neural Networks). The developed system was tested on two databases: DB1 taken from AFORO databases, DB2: a first national otolith databases collected locally in collaboration with INRH (Morocco). The experimental results on DB1 show a significant improvement in recognition rate compared to the previous work of otolith classification. The results on DB2 proved the efficiency and robustness of our approach. Our new automatic classification system of otoliths will help researchers in the fisheries management ecosystem. In future work; we will add other classification features that improve the results for various fish

species which have a high shape similarity. In addition, we will use our approach in the stocks discrimination of fish.

5. References

1 Panfili J, De Pontual H, Troadec H, Wrigh PJ. Manual of fish sclerochronology. Eds, Ifremer, 2003.
2 SCHMIDT W. The otoliths as a means for differentiation between species of fish of very similar appearance. In: Proc. Symp. Oceanog. Fish. Res. Trop. Atl., UNESCO, FAO, OAU, 1969, 393-396.
3 Gaemers PA. Taxonomic position of the Cichlidae (Pisces, Perciformes) as demonstrated by the morphology of their otoliths. Netherlands Journal of Zoology. 1983; 34(4):566-595.
4 L'Abée Lund JH. Otolith shape discriminates between juvenile Atlantic salmon, Salmo salar L., and brown trout, Salmo trutta L. Journal of Fish Biology. 1988; 33(6):899-903.
5 Frost KJ, Lowry UF. Trophic importance of some marine gadids in Northern Alaska and their body-otolith size relationships. Fishery Bulletin. 1981; 79(1):187-192.
6 Nolf D. Otolith piscium, vol. 10 of Handbook of paleoichthyology. Sttutgart and New York: Gustav Fisher Verlag 1985.
7 Lombarte A, Òscar C, Parisi-Baradad V, Roger O, Jaume P, Emilio GL. A web-based environment for shape analysis of fish otoliths. The AFORO database. Scientia marina. 2006; 70(1):147-152.
8 Persoon E, King-Sun F. Shape discrimination using Fourier descriptors. Pattern Analysis and Machine Intelligence, IEEE Transactions, 1986; 3:388-397.
9 TORT A. Elliptical Fourier functions as a morphological descriptor of the genus *Stenosarina* (Brachiopoda, Terebratulida, New Caledonia). Mathematical Geology, 2003; (35)7: 873-885.
10 Duarte-Neto P, Lessa R, Stosic B. The use of sagittal otoliths in discriminating stocks of common dolphinfish (*Coryphaena hippurus*) off northeastern Brazil using multishape descriptors. ICES Journal of Marine Science: Journal du Conseil, 2008; 65(7):1144-1152.
11 Reig-Bolaño R, Marti-Puig P, Lombarte A, Soria JA, Parisi-Baradad V. A new otolith image contour descriptor based on partial reflection. Environmental biology of fishes. 2010; 89(3-4):579-590.
12 Harbitz A, Ole TA. Pitfalls in stock discrimination by shape analysis of otolith contours. ICES Journal of Marine Science: Journal du Conseil. 2015; fsv048.
13 Kuhl, FP, Giardina CR. Elliptic Fourier features of a closed contour. Computer graphics and image processing. 1982; 18(3):236-258.
14 Chuang GC, Kuo CJ. Wavelet descriptor of planar curves: Theory and applications. Image Processing, IEEE Transactions on 1996; 5(1):56-70.
15 Mokhtarian, F, Mackworth A. Scale-based description and recognition of planar curves and two-dimensional shapes. Pattern Analysis and Machine Intelligence, IEEE Transactions on 1986; 1:34-43.
16 Parisi-Baradad V, Lombarte A, García-Ladona E, Cabestany J, Piera J, Chic O. Otolith shape contour analysis using affine transformation invariant wavelet transforms and curvature scale space representation. Marine and Freshwater Research. 2005; 56(5):795-804.
17 Nasreddine K, Benzinou A, Fablet R. Shape geodesics for the classification of calcified structures: beyond Fourier shape descriptors. Fisheries Research. 2009; 98(1):8-15.
18 Parisi-Baradad V, Manjabacas A, Lombarte A, Olivella R, Chic Ò, Piera J, *et al.* Automated Taxon Identification of Teleost fishes using an otolith online database-AFORO. Fisheries Research. 2010; 105(1):13-20.
19 Serra J. Image analysis and mathematical morphology. Academic Press, Inc. 1983.
20 Qingyu G, Chalifour A, Nouboud A, Campeau S, Lavoie I, Mammass D, *et al.* Diatom Classification by Image Analysis, IEEE SETIT, 2004.
21 Williams DR, Hinton GE. Learning representations by back-propagating errors. Nature, 1986, 323-533.
22 Basheer IA, Hajmeer M. Artificial neural networks: fundamentals, computing, design, and application. Journal of microbiological methods. 2000; 43(1):3-31.
23 Reby D, Lek S, Dimopoulos I, Joachim J, Lauga J, Aulagnier S. Artificial neural networks as a classification method in the behavioural sciences. Behavioural processes. 199; 40(1):35-43.